The effects of lightning-produced NOx and its vertical distribution on atmospheric chemistry: sensitivity simulations with MATCH-MPIC

L. J. Labrador, R. von Kuhlmann, M. G. Lawrence

Atmos. Chem. Phys., 5, 1815–1834, 2005
www.atmos-chem-phys.org/acp/5/1815/
SRef-ID: 1680-7324/acp/2005-5-1815
European Geosciences Union

Atmospheric Chemistry and Physics

The effects of lightning-produced NO_x and its vertical distribution on atmospheric chemistry: sensitivity simulations with MATCH-MPIC

L. J. Labrador, R. von Kuhlmann, and M. G. Lawrence

Max-Planck Institute for Chemistry, Department of Airchemistry/NWG, J. J. Becherweg 27, 55128 Mainz, Germany

Received: 6 July 2004 – Published in Atmos. Chem. Phys. Discuss.: 6 October 2004
Revised: 3 June 2005 – Accepted: 7 June 2005 – Published: 22 July 2005

Abstract. The impact of different assumptions concerning the source magnitude as well as the vertical placement of lightning-produced nitrogen oxides is studied using the global chemistry transport model MATCH-MPIC. The responses of NO_x, O_3, OH, HNO_3 and peroxyacetyl-nitrate (PAN) are investigated. A marked sensitivity to both parameters is found. NO_x burdens globally can be enhanced by up to 100% depending on the vertical placement and source magnitude strength. In all cases, the largest enhancements occur in the tropical upper troposphere, where lifetimes of most trace gases are longer and where they thus become more susceptible to long-range transport by large-scale circulation patterns. Comparison with observations indicate that 0 and 20 Tg(N)/yr production rates of NO_x from lightning are too low and too high, respectively. However, no single intermediate production rate or vertical distribution can be singled out as best fitting the observations, due to the large scatter in the datasets. This underscores the need for further measurement campaigns in key regions, such as the tropical continents.

1 Introduction

Nitrogen oxides (NO_x=NO+NO_2) play an important role in tropospheric chemistry. They are catalytic precursors of ozone (O_3) and also have a strong influence on the hydroxyl radical (OH) concentration. Lightning-produced nitrogen oxides constitute an important part of the total NO_x budget, and lightning is one of the sources with the largest uncertainties, with estimates ranging from 1–20 Tg(N)/yr (Lawrence et al., 1995; Price et al., 1997a). Under certain conditions, lightning can compete with anthropogenic sources of NO_x and even be the domintaing source (Zhang et al., 2003a). Produced mostly in and around active thunderstorms, lightning-produced NO_x ($ltNO_x$ hereafter) is readily carried by convective updrafts to the upper troposphere (UT), where its lifetime is considerably longer than in the lower troposphere (LT). The link between lightning and nitrogen oxides was probably first recognized in 1827 by J. von Liebig (von Liebig, 1827), although it was not until the 1970s that further studies were conducted to determine its role in the photochemistry of the LT, primarily in controlling ozone concentrations. $LtNO_x$ is also closely linked with OH radical production and hence has the potential to affect the atmosphere's oxidizing efficiency (Labrador et al., 2004). In order to determine an accurate budget for tropospheric ozone, it is crucial to determine an accurate budget for $LtNO_x$. The large uncertainty in $LtNO_x$ production estimates is reflected in Table 1. From early estimates of the production range exceeding 100 Tg(N)/yr, only in the last decade do we see the estimates in different studies settling within the 1–20 Tg(N) range. While recent studies (e.g.,Huntrieser et al. (2002); Wang et al. (1998)) point towards the lower end of that production range, there is not yet enough solid evidence to discard the upper end thereof. The reasons for this large uncertainty are many-fold; among them, on the one hand, the relatively poorly understood aspects of the lightning phenomenon itself, including the charge separation process, the amount of energy deposited per flash, the partitioning among cloud-to-ground, intracloud and intercloud flashes and, on the other hand, those aspects related to the production of NO_x, such as the amount of NO molecules produced per flash or per unit energy. While a number of laboratory studies have been carried out to determine these parameters, issues such as the similarity of simulated sparks to real flashes and the scalability of laboratory measurements to the characteristic dimensions of the atmosphere may be a source of error. The global distribution of lightning and the total global flash rate continue to be a source of uncertainty, although this has been improved substantially by the recent

Correspondence to: L. Labrador
(lorenzo@mpch-mainz.mpg.de)

Table 1. Global estimates of lightning-produced NO_x (values prior to 1995 adopted from Lawrence et al., 1995).

Reference (type of estimate)	Molec.(NO)/unit energy ($\times 10^{16}$ molec./J)	Molec.(NO)/flash ($\times 10^{25}$ molec./flash)	Number of flashes (flashes/sec)	$LtNO_x$ production rate (Tg(N)/yr)
Tuck (1976)[a]	-	1.1	500	4
Chameides et al. (1977)[a]	3–7	6–14	400	18–41
Noxon (1976)[c]	-	10	500	37
Chameides (1979)[a]	8–17	16–34	400	47–100
Dawson (1980)[a]	-	0.8	500	3
Hill et al. (1980)[a]	-	1.2	100	0.9
Levine et al. (1981)[b]	5±2	0.5	500	1.8±0.7
Kowalczyk and Bauer (1982)[a]	-	10	50	5.7
Peyrous and Lapyere (1982)[b]	1.6	3.2	400	9.4
Drapcho et al. (1983)[c]	-	40	100	30
Chameides et al. (1987)[d]	-	-	-	7
Franzblau and Popp (1989)[c]	-	300	100	220
Sisterson and Liaw (1990)[a]	-	8.2	200	12
Liaw et al. (1990)[e]	-	-	-	81
Lawrence et al. (1995)[e]	-	2.3(1–7)	100(70–150)	2(1–8)
Kumar et al. (1995)[c]	-	0.5	100	2
Ridley et al. (1996)[c]	-	-	100	2–5
Levy et al. (1996)[a]	-	-	-	2–6
Price et al. (1997a)[c]	10	-	70–100	12.2(5–20)
Price et al. (1997b)[a]	10	-	-	13.2(5–25)
Wang et al. (1998)[b]	-	3.1	30–100	2.5–8.3
Nesbitt et al. (2000)[c]	-	0.87–6.2	57	0.9
Navarro-Gonzales et al. (2001)[b]	15±5	-	-	-
Huntrieser et al. (2002)[c]	-	2.7×10^{21} molec/m flash	-	3
Christian et al. (2003)[c]	-	-	44±5	-
Fehr et al. (2004)[c]	-	21	-	-
Ridley et al. (2004)[c]	-	0.3–6.1	-	1.1–19.6

[a] Theoretical estimate
[b] Laboratory-based estimate
[c] Field observations-based estimate
[d] Thunderstorm extrapolation-based estimate
[e] Review-based estimate

advent of dedicated space-borne observation platforms such as the Optical Transient Detector (OTD) and Lightning Imaging Sensor (LIS) (Christian et al., 2003). Airborne observation campaigns provide critically-needed data to help evaluate model results. As will be discussed later, there is a definite need for further measurements of NO_x enhancements in storm areas, particularly in the tropics.

3D global chemistry transport models (CTMs) also constitute useful and powerful tools to study the production of $LtNO_x$ and its potential effects on atmospheric chemistry. In this paper, we study the sensitivity of tropospheric chemistry to various assumptions concerning the vertical placement and source magnitude of $LtNO_x$ using a 3-D CTM. Given the uncertainties mentioned above, it is currently difficult to arrive at definitive conclusions on the effects of these two parameters on the overall contribution of lightning NO_x. In light of this, our main objective with this study is to add to our knowledge about lightning-produced NO_x and its effects with the help of a modeling tool.

This study is broken down as follows; in Sect. 2 a brief description of our model, as well as our approach to modeling the vertical distribution of $LtNO_x$, is laid out. In Sect. 3, the results of model runs with 3 different assumptions concerning the vertical placement of $LtNO_x$ and 5 different total source magnitudes are considered. In Sect. 4 the sensitivity of a number of tropospheric trace gases to different $LtNO_x$ source magnitudes is discussed. In Sect. 5 the results of our different runs are compared with a set of observations for NO_x. Section 6 gives our conclusions.

2 Approach to modeling $LtNO_x$

The model used for this study is the Model of Atmospheric Transport and Chemistry, Max-Planck Institute for Chemistry version, or MATCH-MPIC, an off-line chemistry and transport model based on the NCAR CCM (Community Climate Model) that consists of two main parts, a

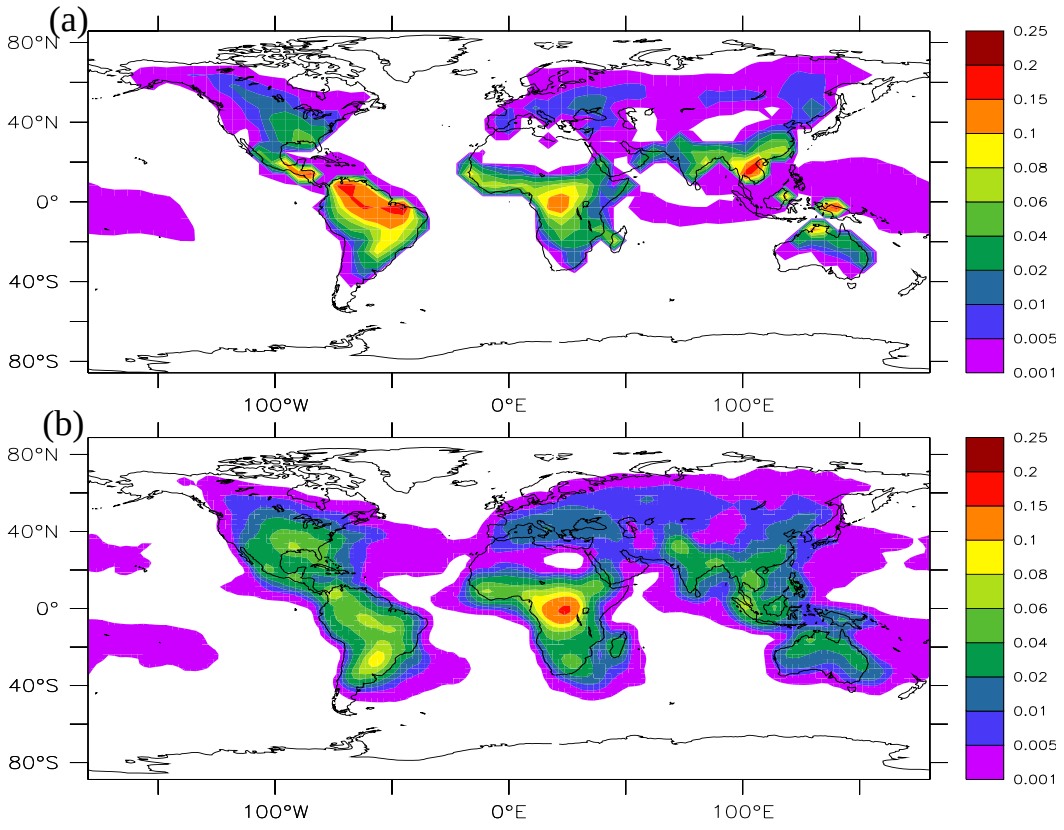

Fig. 1. Averaged flash activity from a)MATCH-MPIC for 1997 and from b)OTD/LIS for 1995–2003 in flashes/km^2/day.

meteorology module and a chemistry module. The chemistry module comprises a suite of 140 gas phase reactions plus one heterogeneous reaction, including the major known sources and sinks of ozone and its associated chemistry as described in detail in von Kuhlmann et al. (2003a). MATCH-MPIC is an off-line model, and therefore needs basic meteorological data as input (temperature, zonal and meridional winds, surface pressure, latent and sensible heat fluxes) to calculate the remaining meteorological parameters, namely vertical wind velocity, convective mass fluxes, cloud fraction and precipitation and vertical turbulence. Two schemes are used to parameterize moist convection; the penetrative deep convection scheme by Zhang and McFarlane (1995), plus the convective adjustment scheme by Hack (1994). The runs for this study were done with input data from the NCEP/NCAR reanalysis at a reduced horizontal resolution of T21 (approximately $5.6°\times5.6°$) and an unchanged vertical resolution which comprises 28 levels, from the surface to 0.2 hPa, in sigma coordinates. The runs were carried out for the year 1997 with a spin-up time of four months. A timestep of 30 min was used. Further details on MATCH-MPIC are in von Kuhlmann et al. (2003a), Lawrence et al. (1999, 2003a), Rasch et al. (1997) and references therein.

2.1 Lightning parameterization

The parameterization for the horizontal distribution of lightning used in MATCH-MPIC is based on Price and Rind (1992)(PR92 hereafter). PR92 developed a simple lightning parameterization based on cloud top height as a predictor of lightning activity. It has been shown that efficient charge buildup and separation processes are strongly dependent on updraft velocity. Cloud top height has in turn been shown to correlate positively with updraft velocity. This, plus the possibility to readily determine cloud top height from direct satellite measurements, was the basis for choosing it as a first suitable predictor of lightning activity. The parameterized relationship between cloud top height and flash frequency is: $F=3.44\times10^5\,H^{4.9}$ for continental convective clouds, and $F=6.4\times10^4\,H^{1.73}$ for marine clouds, where F is the flash frequency (in flashes/min/$8°\times10°$ box) and H is the modeled cloud top height (in km). Figure 1 shows the averaged global lightning distribution using PR92 in MATCH-MPIC for the year 1997 and as observed by the OTD and LIS for the the period from mid 1997 to early 2003. The observed lightning distribution was made using a composite dataset that makes it possible to combine the larger spatial coverage of the OTD and the longer timespan and better detection efficiency of the LIS. The model captures the main features and the general

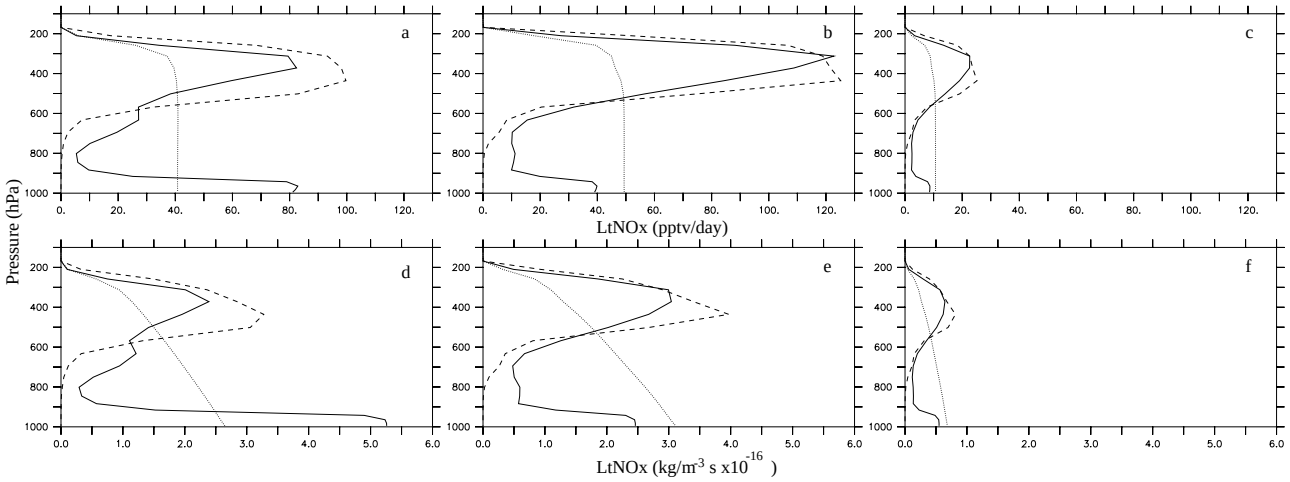

Fig. 2. Monthly mean $LtNO_x$ emissions, from model output, in pptv/day **(a–c)** and 10^{-16}kg/m^{3}s **(d–f)**, for the three vertical distributions in this study: PICK (solid line), ANVIL (dashed line) and EVEN (dotted line), at selected locations representative of the PICK distribution's three cases: (a) and (d) midlatitude continental (35° N, 90° W for June 97); (b) and (e) tropical continental (8° N, 65° W for July 1997) and (c) and (f) tropical marine (12° N, 63° W for July 1997).

Table 2. MATCH-MPIC runs done for this study.

Run	$LtNO_x$ production (Tg(N)/yr)	Vertical distribution
$NoLtNO_x$	0	N/A[a]
EVEN2	2	Density-weighted[a]
EVEN5	5	Density-weighted[a]
EVEN10	10	Density-weighted[a]
PICK2	2	Pickering et al. (1998)
PICK5	5	Pickering et al. (1998)
PICK10	10	Pickering et al. (1998)
PICK20	20	Pickering et al. (1998)
ANVIL2	2	Five uppermost layers of cloud
ANVIL5	5	Five uppermost layers of cloud

[a] Constant mixing ratio in the vertical

pattern of the observed flash distribution well. The flash activity over the southeastern United States is well reproduced, as is the overall pattern over India and southeastern Asia. However, an overestimation of the flash activity is apparent over the tropics, particularly over northern and central South America, Central America, southeastern Asia, eastern India, eastern Borneo, Papua-New Guinea and northern Australia. On the other hand, flash activity is underestimated mostly over the extratropics, particularly over the Western and South Western United States, the Mediterranean basin, parts of central Europe and the Caucasus range, the Middle East, Central and South-Central Asia, north-eastern China and southern Australia. Most of the activity over Indonesia is underestimated, except for easternmost Borneo. The strong signal over the Congo basin is well reproduced except for some underestimation at the center of the feature. Coastal lightning is mostly underestimated by the model as is marine lightning, particularly over the North and South Atlantic and the northwestern Pacific. While these discrepancies might be a result of the lightning parameterization itself, other factors, such as the convection parameterization used and the model's failure to reproduce off-shore transport of lightning-active convective clouds, may also play a role. In the last few years, other lightning parameterizations have been proposed, particularly focusing on using convective mass fluxes (e.g., Allen and Pickering (2002)); the use of these in MATCH-MPIC is being examined in a parallel study.

2.2 Vertical distribution of $LtNO_x$ in MATCH-MPIC

In previous versions of MATCH-MPIC, $LtNO_x$ was input as a uniform volume mixing ratio throughout the vertical convective column. This was chosen based on three assumptions; first, intracloud flashes are much more frequent than cloud to ground flashes (Price and Rind, 1994). Second, cloud to ground discharges are much more energetic than intracloud discharges (Turman, 1978; Kowalczyk and Bauer, 1982) and third, NO_x production by lightning apparently exhibits a strong dependence on the ambient air density, being less for lower densities (Goldenbaum and Dickerson, 1993). The first two can be regarded as canceling each other out to an extent. The third assumption then results in an approximately even mixing ratio (i.e., density-weighted) distribution of the emissions in the vertical. The first and third assumptions can also be regarded as canceling each other out, even in the event that intra cloud discharges might be as effective in producing NO_x as cloud to ground discharges, as suggested by Gallardo and Cooray (1996); Cooray (1997); DeCaria et al. (2000) and Fehr et al. (2004). While these assumption

are hard to prove or disprove, there is recent evidence that the vertical distribution of $LtNO_x$ in deep-convective clouds is likely to be quite different from an even mixing ratio in the vertical. Pickering et al. (1998) (subsequently P98) used a cloud-resolving model to develop a set of profiles to typify the vertical distribution of $LtNO_x$ after a convective storm for use in specifying the effective lightning NO_x source in global and regional chemistry models. Profiles were computed for three different regimes: tropical continental, tropical marine and mid-latitude continental. We have implemented all three profiles from P98 in MATCH-MPIC and, since a midlatitude marine profile was not developed in P98, we adopted the midlatitude continental profile for all midlatitude areas, marine areas included. The profiles were scaled (stretched or squeezed in the vertical) to fit the depth of convection in each model column.

A recent study by Zhang et al. (2003b) has shown that simulations of different storms can lead to qualitatively similar but quantitatively different profiles from P98. Thus, more work is needed to determine the most appropriate assumptions for use in global models. Here we examine the basic sensitivity of the simulated tropospheric chemistry to various assumed profiles of $LtNO_x$, which provides an indication of the degree of importance of refining the knowledge and parameterizations of its vertical placement.

2.3 Sensitivity studies

In order to assess the impact of $LtNO_x$ and its vertical placement on tropospheric chemistry, a set of sensitivity runs was carried out where a number of different assumptions concerning the source strength and the vertical distribution of the lightning NO_x source were implemented, as summarized in Table 2.

First, a run in which the lightning NO_x source was turned off (NoLtNO_x run) was carried out. Although a zero $LtNO_x$ production rate is not realistic, this run serves as a *Gedanken-experiment* against which to compare other runs, in order to be able to assess the net impact of the lightning NO_x source on the model's NO_x distribution and budget.

Second, a series of runs with various $LtNO_x$ source magnitudes was done with 3 vertical distributions: 1) a density-weighted distribution as in previous versions of MATCH-MPIC, from cloud top to ground (or cloud bottom over the oceans), which we will refer to as the EVEN distribution; 2) the distribution according to the vertical profiles developed by Pickering et al. (1998), hereafter referred to as the PICK distribution; 3) a distribution in which all of the $LtNO_x$ is deposited in the five top-most layers of the convective column, intended to represent the upper limit of upward transport of $LtNO_x$ by convective updrafts which we will call the ANVIL distribution.

The mean vertical $LtNO_x$ profiles based on these three assumptions are plotted in Fig. 2 for a run with a source strength of 2 Tg(N) of NO_x from lightning, and the percentage of total NO_x deposited by each distribution at specific pressure levels is shown in Table 3. The EVEN distribution simulates an even-mixing ratio profile in the vertical, which means decreasing fluxes with altitude. In the three different profiles, the EVEN distribution exhibits remarkably similar fluxes over the same pressure intervals, in a behavior consistent with a prescribed constant mixing ratio. The largest influx of $LtNO_x$ into the UT from this distribution occurs in the tropical continental case, due to convection reaching the highest altitudes in the tropics. The PICK distribution simulates the largest fluxes in the 1000–800 and 500–300 hPa regions. This is consistent with both the prescription of 20% of the total $LtNO_x$ mass deposited in the lowest levels for the midlatitude continental case and with strong convection present in the midlatitudes, respectively. Conversely, this distribution shows the lowest fluxes in the 800–500 hPa layer. In the tropical continental case, the PICK distribution simulates almost similar fluxes in both the 1000–800 and 800–500 hPa ranges and the largest fluxes in the 500–300 hPa layer. The tropical continental case simulates, in fact, the largest fluxes in this pressure range of all three cases, due to the depth of convection in the tropics as well as the higher tropopause there. In the tropical marine case, where downdrafts are not that strong, the PICK distribution shows the lowest fluxes in the 1000–800 hPa layer, lower even that in the 800–500 hPa layer. The tropical marine case simulates the lowest fluxes of all three distributions in both the 500–300 and 300–100 hPa layers. Though the tropopause is high in the tropics, convection over oceanic regions is not as strong as over the continents, resulting in decreased fluxes. The ANVIL distribution simulates the largest fluxes in the 500–300 hPa layer in all 3 cases, consistent with the $LtNO_x$ being placed in the five

Table 3. Vertical distribution, in percentage of total $LtNO_x$, of the different vertical profiles at different pressure levels.

	EVEN	PICK	ANVIL
Midlat. continental			
1000–800	36.4	36.9	0.1
800–500	41.7	2.2	0.2
500–300	18.2	54.3	85.2
300–100	3.7	6.6	14.5
Trop. continental			
1000–800	35.9	21.3	0.02
800–500	41.1	19	12.9
500–300	18	45.1	66
300–100	5	14.6	21.1
Trop. marine			
1000–800	38.1	20.7	0.3
800–500	43.7	33.7	46.1
500–300	17.1	43.5	50.1
300–100	1.1	2.1	3.5

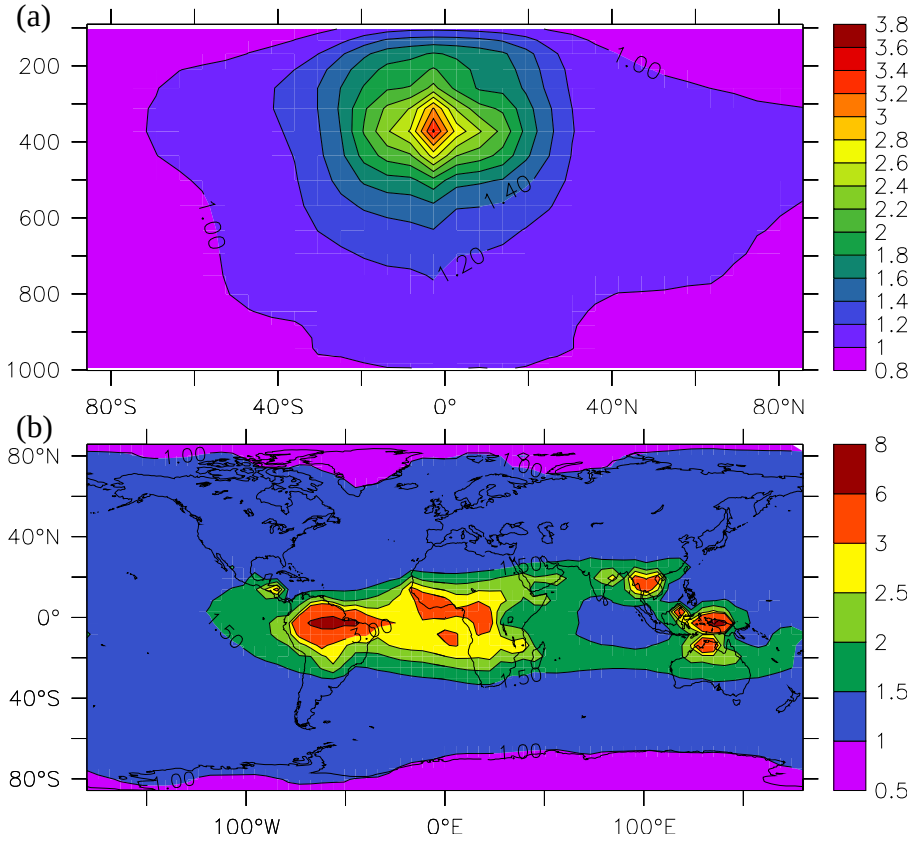

Fig. 3. Ratio of **(a)** annual zonal means and of the **(b)** horizontal distributions at 300 hPa of NO_x for the PICK5 and $NoLtNO_x$ runs.

uppermost model levels of the convective column. Almost no fluxes are simulated in the lowermost layer in this distribution. In the 300–100 hPa layer, the simulated fluxes in the ANVIL distribution are twice as large as the PICK fluxes in the midlatitude continental case, 60% larger in the tropical continental case and 75% larger in the tropical marine case. The amount of NO_x deposited at the higher levels is a critical parameter in model simulations. According to Ridley et al. (2004) the correct injection of NO_x in the UT is far more important than in the middle troposphere, since its lifetime at lower altitudes is shorter.

Different $LtNO_x$ source magnitudes, spanning the currently accepted range of uncertainties in the source, were used for these distributions. A series of runs with $LtNO_x$ production rates of 2, 5, and 10 Tg(N)/yr using the EVEN distribution (hereafter EVEN2, EVEN5 and EVEN10, respectively) were carried out. Similarly, runs with $LtNO_x$ production rates of 2, 5, 10 and 20 Tg(N)/yr using the PICK distribution (hereafter PICK2, PICK5, PICK10 and PICK 20, respectively) and $LtNO_x$ production rates of 2 and 5 Tg(N)/yr using the ANVIL distribution (ANVIL2 and ANVIL5, respectively) were also made. This results are then compared to the $NoLtNO_x$ run. This information is summarized in Table 4. The largest source (20 Tg(N)/yr), which we consider to be relatively unlikely, was only examined for the "best" vertical distribution (i.e, PICK20). In this study, we will analyze the effects of these different vertical distributions and source magnitudes on NO_x, O_3, OH, HNO_3 and peroxyacetyl nitrate (PAN, hereafter). We will focus our discussion on the PICK5 run, since it best reflects the currently accepted estimate for $LtNO_x$ and the most physically-based vertical distribution in the literature.

3 Significance of $LtNO_x$ for tropospheric NO_x concentrations

In this section, we will analyze the significance of the source of NO_x from lightning on total NO_x concentrations. To that end, we will compare the results of the PICK5 run (i.e., our reference run) against the $NoLtNO_x$ run. Fig. 3a and b depict the ratio of the annual zonal means of the PICK5 vs $NoLtNO_x$ runs, and the ratio of the horizontal NO_x distributions at 300 hPa, respectively. Most of the enhancement due to $LtNO_x$ takes place in the tropical mid and upper troposphere, mainly between 40° north and south latitude and between 800 and 200 hPa. A 20% enhancement in the zonal mean mid- and upper troposphere is evident at 700 hPa, peaking at approximately 300 hPa over the equator,

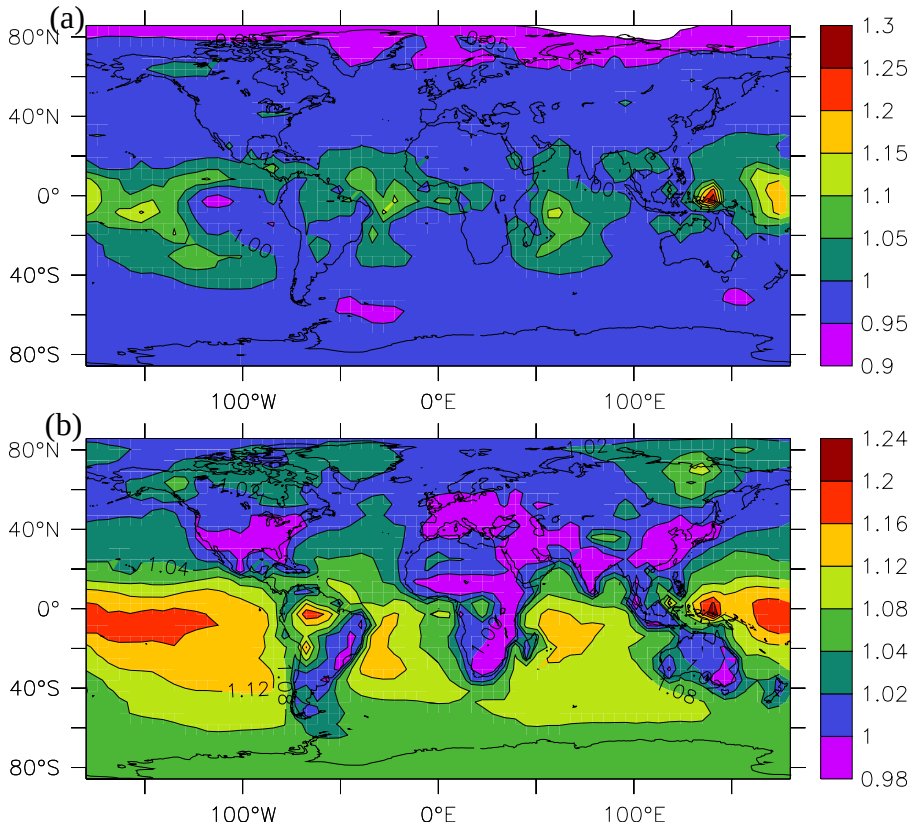

Fig. 4. Ratio of the horizontal distributions at 1000 hPa of **(a)**NO_x and **(b)**OH for the PICK5 and $NoLtNO_x$ runs.

where a factor of 3.4 more NO_x is present compared to the $NoLtNO_x$ run. The largest enhancements in the tropical UT are consistent with lightning activity being prevalent over the tropics and continental regions (Christian et al., 2003), especially over equatorial South America, central Africa, and Indonesia. However, based on the preliminary evaluation discussed above, comparisons with OTD data indicate that the enhancements in NO_x might be biased high due to a tendency of the lightning parameterization to overestimate flash activity in the tropics. We see that, despite the fact that the PICK5 vertical distribution of $LtNO_x$ prescribes around 20% of the total $LtNO_x$ to be released in the first 2 km above the continental landmasses, the enhancement there is relatively small. This is mainly due to the fact that, at surface levels, $LtNO_x$ must compete against other surface sources, such as soils, biomass burning and urban and industrial fossil fuel burning emissions.

Interestingly, the addition of $LtNO_x$ causes surface total NO_x mixing ratios to decrease by ∼5%, particularly over the extratropical LT (Fig. 4a). Stockwell et al. (1999) found the same result, particularly over Europe and North America, and attributed it to increases in OH due to the general increase in O_3 when lightning is included in their model simulations. There are two mechanisms to account for the computed NO_x losses, namely the reaction of OH with NO_2 to form HNO_3 and the conversion of N_2O_5 into HNO_3 via hydrolysis on aerosols. Figure 4b shows the annual mean surface ratio of OH for the PICK5 and the $NoLtNO_x$ runs. A general decrease of ∼2% in surface OH is simulated over most midlatitude and some tropical landmasses when $LtNO_x$ is included in our simulations, mainly between 50° north and 40° south, rendering the first mechanism unsuitable to explain the loss (NO_2 levels do increase slightly but not enough to compensate for the decrease in OH). The explanation of Stockwell et al. (1999) can be used to interpret our results outside of that latitude range where, in our simulations, surface OH increases when adding $LtNO_x$. However, wherever there is a decrease in surface OH, the negative NO_x feedback can only be explained by an increase in the NO_x loss rate via the second loss reaction. This mechanism depends partly on O_3 levels, which control the formation of NO_3 and therefore N_2O_5. We compute an increase in surface O_3 concentration of ∼3% for the midlatitude continental areas (not shown), largely due to downward convective mixing of O_3 produced by $LtNO_x$ aloft (Lawrence et al., 2003b). This enhances the loss of NO_y via hydrolysis of N_2O_5, and ultimately leads to the computed reduction in NO_x levels.

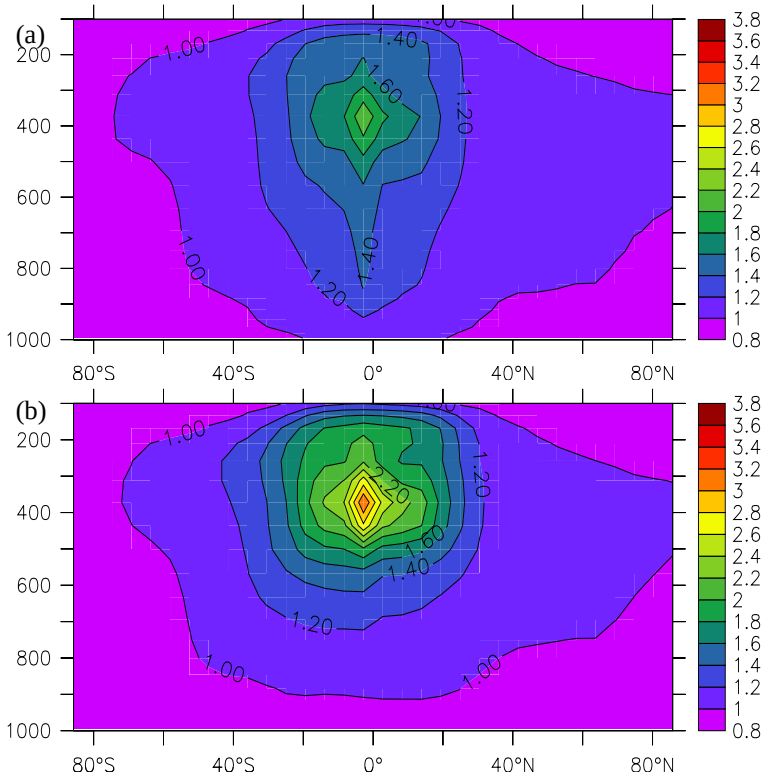

Fig. 5. Ratios of the annual zonal means of the **(a)** EVEN5 and **(b)** ANVIL5 runs to the $NoLtNO_x$ run for total NO_x.

4 Effects of the different assumptions of vertical placement of $ltNO_x$ on the vertical distribution of different trace gases

What is the impact of the different assumed vertical distributions of $LtNO_x$ on atmospheric chemistry? In order to answer this question, we compare the effects of the three main vertical distributions tested in this study for the 5 Tg(N)/yr source, i.e. EVEN5, PICK5, and ANVIL5, against the $NoLtNO_x$ run. We consider NO_x as well as O_3, OH, HNO_3 and PAN. Common to all three distributions is that the largest enhancement in all of these species occurs in the tropical UT, between approximately 500 and 300 hPa, with the main differences being in the magnitude and the vertical extent of the enhancement.

The EVEN5 distribution results in a gradual enhancement in NO_x with altitude (Fig. 5a), consistent with a density-weighted distribution, reaching a maximum of a factor of 2 higher than the $NoLtNO_x$ run between approximately 300 and 400 hPa above the equator. This is quite different than the PICK5 and ANVIL5 runs (Figs. 3a and 5b, respectively), which simulate very similar enhancements to each other, although the ANVIL5 run, more weighted toward the UT, simulates a reduction below 900 hPa at all latitudes and no evident enhancement below 800 hPa. The maximum enhancement in these two runs is about a factor of 3 higher than the mixing ratio of the $NoLtNO_x$ run at 300–400 hPa and represents a 100% larger enhancement than computed for the EVEN5 distribution. Considering that all three runs were done with the same 5 Tg(N)/yr $LtNO_x$ production rate, this is a significant result, since accounting for the lofting by convective updrafts in the PICK5 and ANVIL5 runs results in twice the enhancement of NO_x in the UT compared to the EVEN distribution. In all three runs, decreases in total NO_x are computed at the surface in the extratropics and even in the tropics in the ANVIL5 run. As discussed before, this is mainly due to downward transport of ozone produced by enhanced NO_x in the UT, reducing the near-surface NO_x lifetime

Much like with NO_x, a gradual vertical enhancement of O_3 is simulated in the EVEN5 run (Fig. 6a), with the largest enhancements occurring at the tropical latitudes (in contrast to the reduction in surface NO_x at high latitudes). Surface enhancements range from 12% within the tropics to ∼4% at high latitudes. The peak enhancement is approximately 30% between 200 and 700 hPa in the tropics. Again, the PICK5 and ANVIL5 runs (Figs. 6b and c, respectively) simulate very similar profiles except at the surface, where the PICK5 run results in an enhancement of up to 15% close to the equator and ∼10% in the tropical regions, compared to a maximum zonal mean near-surface enhancement of 10% in the ANVIL5 run for most of the tropics. The largest

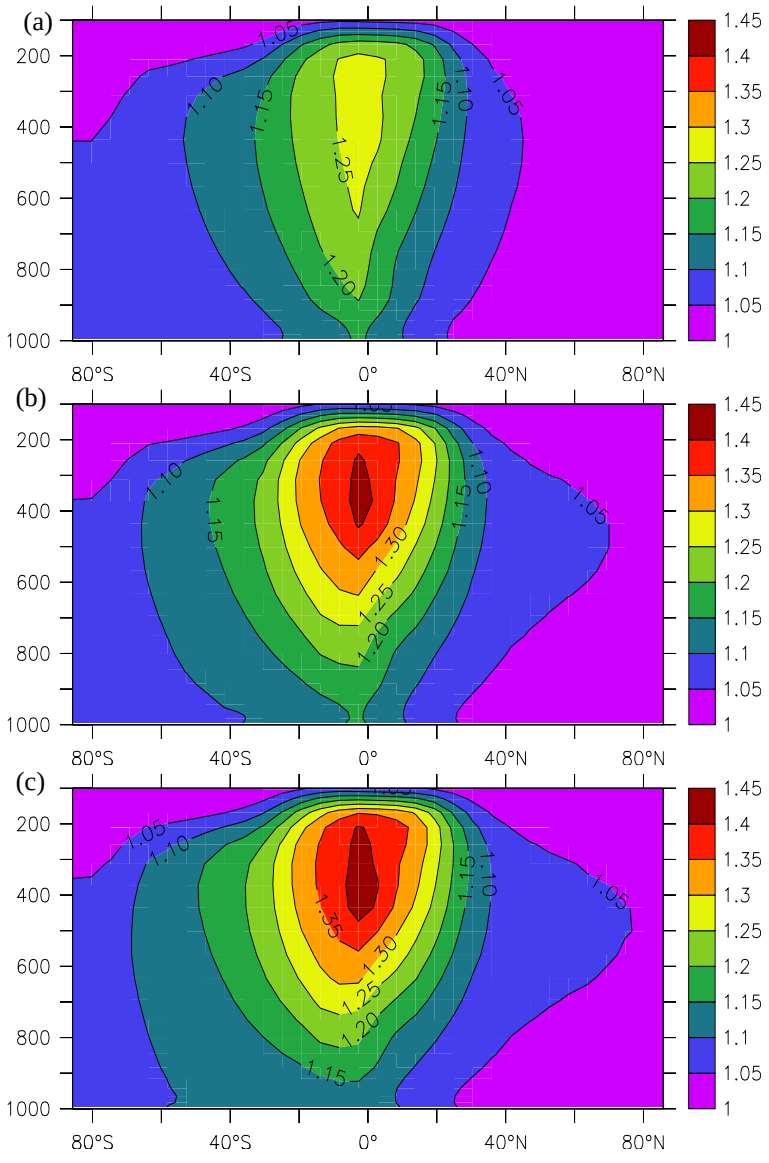

Fig. 6. Ratios of the annual zonal means of the **(a)** EVEN5, **(b)** PICK5 and **(c)** ANVIL5 runs to the $NoLtNO_x$ run for O_3.

enhancements in both runs are simulated between 200 and 400 hPa over the tropics with 45% more O_3 compared to the $NoLtNO_x$ run. The general differences in tropospheric O_3 as a result of the different vertical placements emphasize the role of NO_x in controlling the O_3 budget, and underscores the need not only to determine an accurate estimate of the $LtNO_x$ source magnitude, but also to correctly assess its post-storm vertical distribution.

There is a significant impact on OH by $LtNO_x$. In the EVEN5 run (Fig. 7a), enhancements of up to 60% with respect to the $NoLtNO_x$ run are simulated in the tropical UT, mainly in the altitude band between 300 and 100 hPa. Again the PICK5 and ANVIL5 runs (Figs. 7b and c, respectively) show very similar profiles for OH, with enhancements of approximately 100% between 100 and 200 hPa. All three runs also simulate enhancements of about 10% near surface levels in the tropics. The enhancements in the cold and dry tropical UT are because there production of OH via $O(^1D)+H_2O$ is slow, while secondary sources, such as enhancements in HO_x recycling efficiency due to increased NO_x, take on a more important role. Despite the strong temperature dependence of the oxidation reactions of long-lived trace gases such as methane and methylchloroform, this result has an important effect on the oxidizing efficiency of the troposphere, and increases in the source magnitude of $LtNO_x$ can lead to a substantial reduction in the computed lifetimes of these trace gases (Labrador et al., 2004).

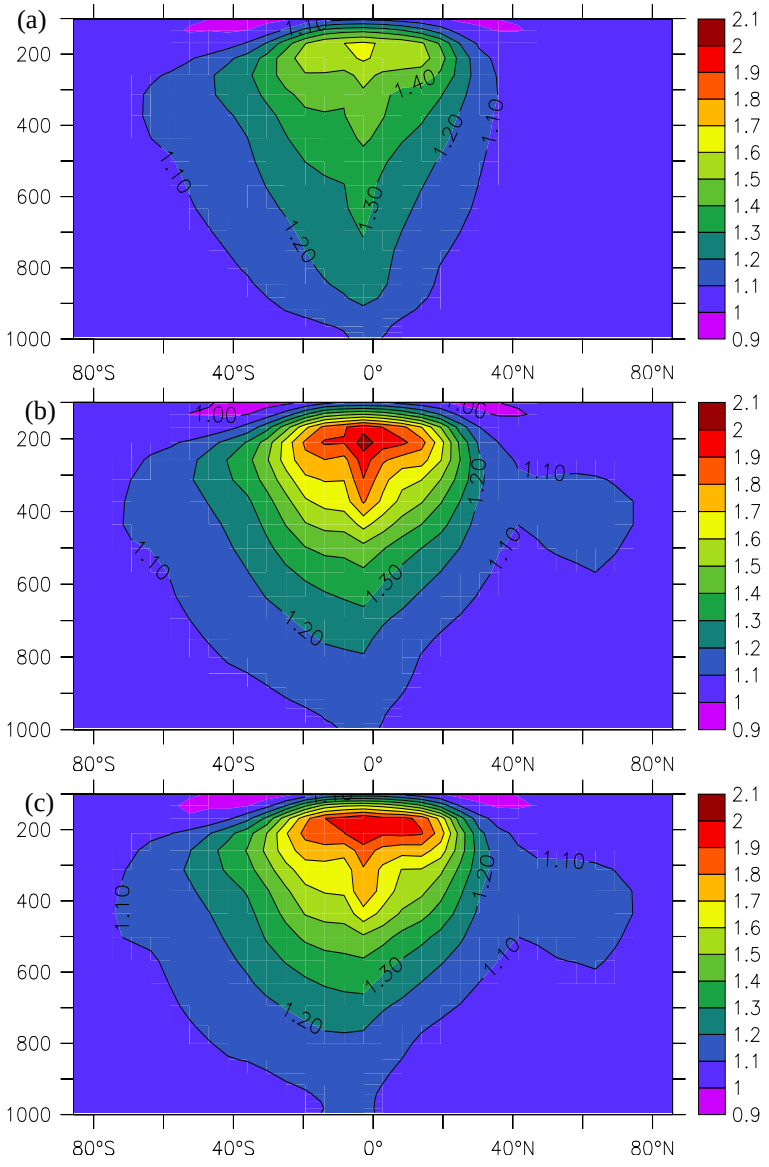

Fig. 7. Ratios of the annual zonal means of the **(a)** EVEN5, **(b)** PICK5 and **(c)** ANVIL5 runs to the $NoLtNO_x$ run for OH.

There is a very sensitive response of nitric acid, one of the main reservoirs through which reactive nitrogen is lost (via dry and wet deposition), to $LtNO_x$. All three distributions simulate enhancements greater than a factor of 2 with respect to the $NoLtNO_x$ run, as can be seen in Figs. 8a, b and c. The particularly sensitive response is due to the fact that, on adding $LtNO_x$, not only NO_2, a direct precursor of nitric acid, but also another precursor, OH, is enhanced. From all three distributions, it can be observed that, compared to most other trace gases discussed, the maximum enhancements in nitric acid occur at a somewhat lower altitude i.e., between 400 and 500 hPa. Two main reasons could account for this fact: first, while the largest relative increase in OH by adding $LtNO_x$ occurs in the UT, the largest absolute enhancement occurs at a lower altitude (Labrador et al., 2004), coinciding with the maximum enhancement in nitric acid. Furthermore, in the UT, there is a buffering effect of PAN, which is enhanced at the expense of nitric acid. The PICK5 and ANVIL5 runs (Figs. 8b and c, respectively) are very similar, although the enhancement in the UT at higher latitudes is greater in the ANVIL5 run and the PICK5 run simulates larger enhancements than the ANVIL5 run in the lowermost levels.

The importance of the NO_x reservoir species peroxyacetyl nitrate (PAN) lies in its high stability at low temperatures. Once produced, it can be transported long distances and, through thermal degradation, it can introduce NO_x into remote regions, where background levels are generally low. As

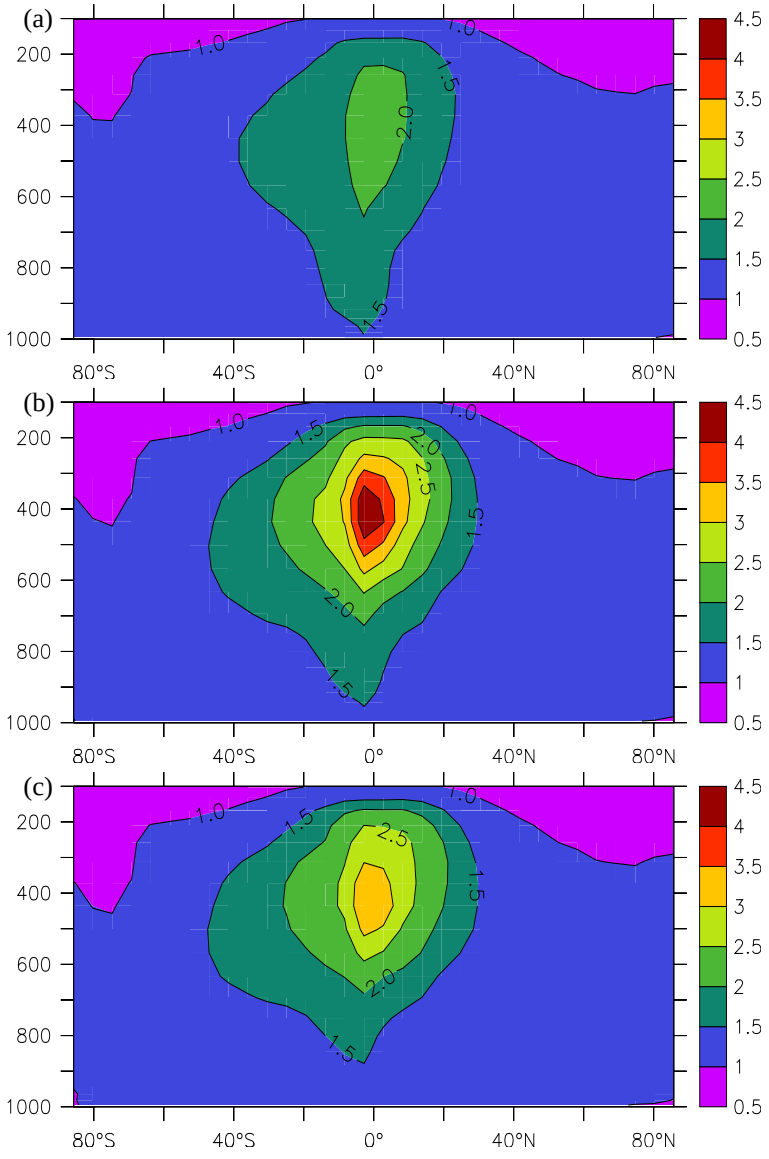

Fig. 8. Ratios of the annual zonal means of the **(a)** EVEN5, **(b)** PICK5 and **(c)** ANVIL5 runs to the NoLtNO$_x$ run for HNO_3.

shown in Figure 9a, the burden of PAN is doubled in the tropical UT by assuming the PICK5 lightning NO_x vertical distribution. The EVEN5 run (Fig. 9a) simulates increases of over 50% from 500 hPa up to the tropopause level over the tropics, where values peak at a factor of 1.6 larger than the NoLtNO$_x$ run. The PICK5 and ANVIL5 runs (Figs. 9b and c, respectively) show again a very similar pattern. Maximum enhancements are of the order of 100% between ∼300 and 200 hPa in both distributions, with enhancements decreasing rapidly outside of the tropical latitudes. All three distributions simulate enhancements in PAN in the UT, as a result of increases in total NO_x in the same region. The ANVIL5 run simulates no notable enhancement at the surface, whereas the PICK5 run shows a 10% enhancement, consistent with the placement of NO_x by the PICK98 profiles in the lowermost troposphere.

5 Sensitivity of tropospheric trace gas burdens to the increase in the source of NO_x from lightning

In this section, we analyze the responses of NO_x, as well as O_3, OH, HNO_3 and PAN to increases in the source magnitude of LtNO$_x$. We calculated the burdens of these trace gases for the whole globe (90° north to 90° south), the tropics (between 25° north and south), and the extratropics (90° to 25° north and 25° south to 90° south), for the EVEN2, 5 and 10 and PICK2, 5, 10 and 20 runs . Since the PICK and

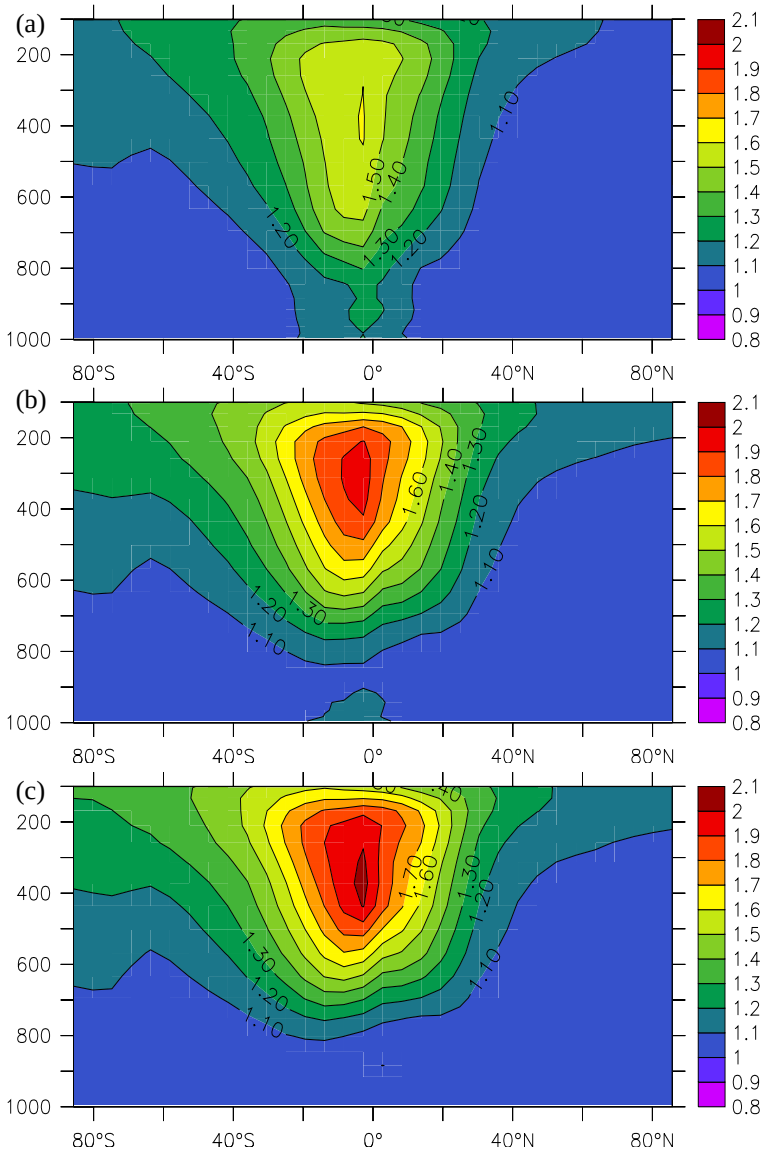

Fig. 9. Ratios of the annual zonal means of the **(a)** EVEN5, **(b)** PICK5 and **(c)** ANVIL5 runs to the NoLtNO_x run for PAN.

ANVIL runs produce mostly similar results, we will limit our comparison to the EVEN and PICK set of runs.

Figures 10a–e show the burdens for the EVEN and PICK runs as a function of the LtNO_x source magnitude. A consistent tendency was for the PICK runs to result in higher burdens for all trace gases than the EVEN runs, due to their lifetimes generally being longer in the UT, where most of the NO_x in the PICK runs is released.

Globally, adding LtNO_x produces a tendency towards saturation, already seen from 2 Tg(N)/yr–5 Tg(N)/yr and which becomes very clear in the 20 Tg(N)/yr production rate. The response of the EVEN set of runs is similar to the PICK runs, although the magnitude of the absolute increase in total NO_x is not as marked as that of the PICK runs. Interestingly, the difference in the total NO_x burden for equivalent production rates between the PICK and EVEN runs increases with increasing LtNO_x: relative to the NO LtNO_x run, the PICK2 run simulates a total NO_x burden 2.5% larger than the EVEN2 run. For the 5 and 10 Tg(N)/yr production rates, these differences are 4.3 and 5.3%, respectively. This is a consequence of the weighting of the PICK distribution towards the higher altitudes, as opposed to the density-weighted EVEN distribution.

The tropical regions simulate a more sensitive response, due in large part to the fact that most of the lightning activity in the model is concentrated there (Fig. 1) and because the other competing sources (especially fossil-fuel burning) tend to be smaller in the tropics than in the extratropics. Though

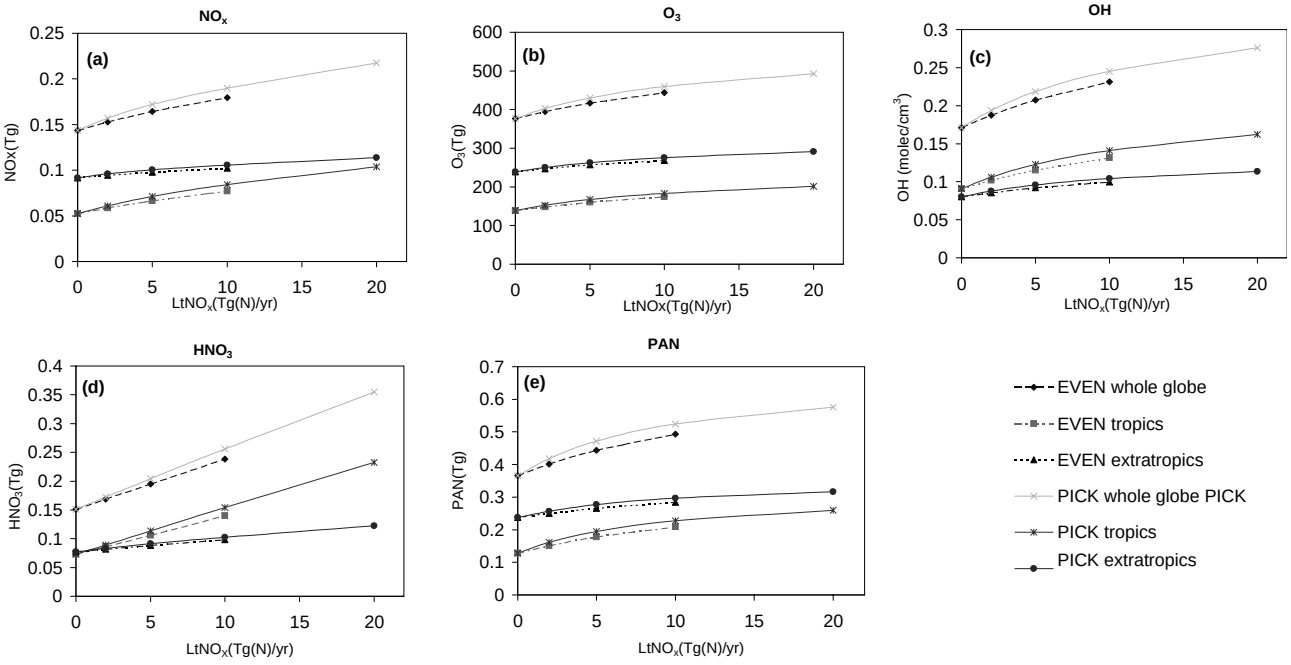

Fig. 10. Burdens of **(a)** NO_x, **(b)** O_3, **(c)** OH, **(d)** HNO_3 and **(e)** PAN, for the PICK and EVEN series of runs for the tropics and extratropics.

Table 4. Burdens of the NoLtNO$_x$ runs (in Tg for NO_x and O_3 and $\times 10^6$ molec for OH) and relative increases (in percent) of the burdens of the different trace gases for the whole globe and tropics (T) for the different runs with respect to the LtNO$_x$ runs.

Trace	Burden in	Relative increase vs. NoLtNO$_x$ run						
gas	NoLtNO$_x$ run	P2	P5	P10	P20	E2	E5	E10
NO_x	0.14	9.1	19.5	31.9	51.2	6.4	14.4	24.9
NO_x(T)	0.05	16.6	36.4	60.6	98.2	11.9	27.3	47.8
O_3	377.1	6.8	14.1	21.8	30.7	4.9	10.6	17.6
O_3 (T)	138.5	9.9	20.8	32.3	45.6	7.1	15.7	26.2
OH	0.17	13.2	27.8	43.1	61.3	9.6	21.1	35.1
OH (T)	0.09	16.4	34.8	54.8	78.4	11.9	26.5	44.6
HNO_3	0.15	14.2	35.6	69.6	135.2	11.6	29.1	59.8
HNO_3 (T)	0.07	21.4	54.7	109.6	217	17.6	44.7	90.7
PAN	0.37	14.2	28.9	43.2	57.4	9.7	21.3	34.9
PAN (T)	0.13	8.1	51.7	24.8	33.2	5.5	12.0	19.8

the same non-linear response as in the whole globe is also present, increases in total NO_x in the tropics are larger. The differences in burden growth with respect to the NoLtNO$_x$ run between the PICK and EVEN runs are also larger than in the whole globe: 4%, 6.7% and 7.9% for the 2, 5 and 10 Tg(N)/yr production rates, respectively.

As with NO_x, O_3 shows a non-linear response to increases in LtNO$_x$, tending towards saturation at the highest end of the range in both sets of runs. The PICK runs simulate larger enhancements throughout the entire production range, particularly in the tropical regions (Fig. 10b and Table 4). Globally, the PICK20 run simulates increases of up to 30% with respect to the NoLtNO$_x$ run, while in the tropics O_3 is enhanced by 45% for the same run. These enhancements are all the more important considering that they take place in the UT, where longer lifetimes and the Hadley circulation can transport this ozone to higher latitudes and because O_3 is more efficient as a greenhouse gas at higher altitudes. This increase of O_3 at higher altitudes is responsible for the reduction of surface NO_x levels simulated at high latitudes in Fig. 4a.

Table 5. Regional annual mean airmass-weighted OH concentrations ($\times 10^6$ molec/cm^3) and relative increases vs. $NoLtNO_x$ (in parenthesis) for the different $LtNO_x$ vertical distributions.

REGION	$NoLtNO_x$	EVEN5	PICK5
Below 750 hPa 90° S–30° S	0.54	0.58 (+7.4%)	0.59 (+9.3%)
Below 750 hPa 30° S–0°	1.25	1.45 (+16%)	1.43 (+14.4%)
Below 750 hPa 0°–30° N	1.44	1.59 (+10.4%)	1.56 (+8.3%)
Below 750 hPa 30° N–90° N	0.82	0.85 (+3.7%)	0.85 (+3.7%)
750–500 hPa 90° S–30° S	0.48	0.55 (+14.6%)	0.56 (+17%)
750–500 hPa 30° S–0°	1.21	1.53 (+26.4%)	1.56 (+28.9%)
750–500 hPa 0°–30° N	1.44	1.71 (+18.8%)	1.72 (+19.4%)
750–500 hPa 30° N–90° N	0.72	0.77 (+6.9%)	0.77 (+6.9%)
500–250 hPa 90° S–30° S	0.34	0.40 (+17.6%)	0.42 (+23.5%)
500–250 hPa 30° S–0°	0.67	0.93 (+38.8%)	1.07 (+59.7%)
500–250 hPa 0°–30° N	0.87	1.13 (+29.9%)	1.27 (+46%)
500–250 hPa 30° N–90° N	0.52	0.57 (+9.6%)	0.58 (+11.5%)

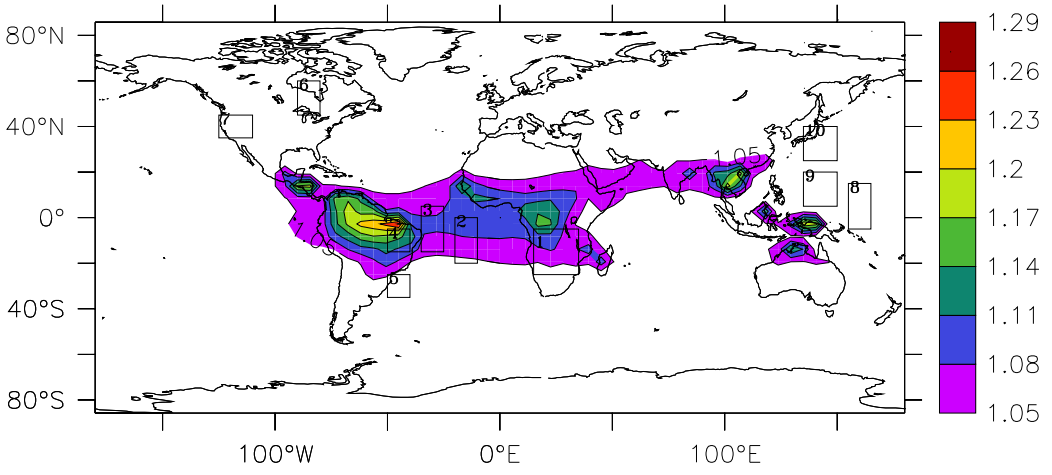

Fig. 11. Campaign regions (within boxes), superimposed on the ratio of the annual horizontal distribution of NO_x from the PICK5 and $NoLtNO_x$ runs.

Figure 10c shows that the relative change in global enhancement of the OH burden is greater than that of O_3 and is close to that of NO_x. Table 5 shows the regional annual mass-weighted OH mean concentrations, as suggested by Lawrence et al. (2001), for the different vertical distributions with a 5 Tg(N)/yr $LtNO_x$ production rate, as well as the relative increases of the two vertical distributions versus the $NoLtNO_x$ run. The largest OH increases in all three distributions are in the southern hemisphere, despite the lightning activity being dominant over the northern hemisphere (Christian et al., 2003). For instance, in the EVEN5 distribution, the enhancements in the 90° S–30° S domains at all altitudes are about a factor of two larger than those in the equivalent domains in the northern hemisphere, whereas in the 30° S–0° domains, they are about 50% larger than in the 0°–30° N domains. In the PICK distribution the enhancements in the 90° S–30° S regions below 750 hPa are a factor of three larger, and in the 750–500 hPa and 500–250 hPa domains approximately a factor of two larger than the equivalent northern hemisphere domains. In the 30° S–0° domains, the enhancements are about 50% larger than in the 0°–30° N domains. This marked sensitivity of the southern hemisphere to $LtNO_x$ is a result of lower total NO_x emissions from other sources, which makes OH more sensitive to increases in NO_x there. The PICK distribution simulates larger relative increases vs. the $NoLtNO_x$ run in the uppermost domains than the EVEN distribution, particularly in the tropics, consistent with the larger amounts of $LtNO_x$ deposited in the upper levels by the PICK distribution.

Nitric acid (HNO_3) (Fig. 10d) shows a marked sensitivity to increases in $LtNO_x$ which is different from the other gases. There is more than a doubling in its burden between

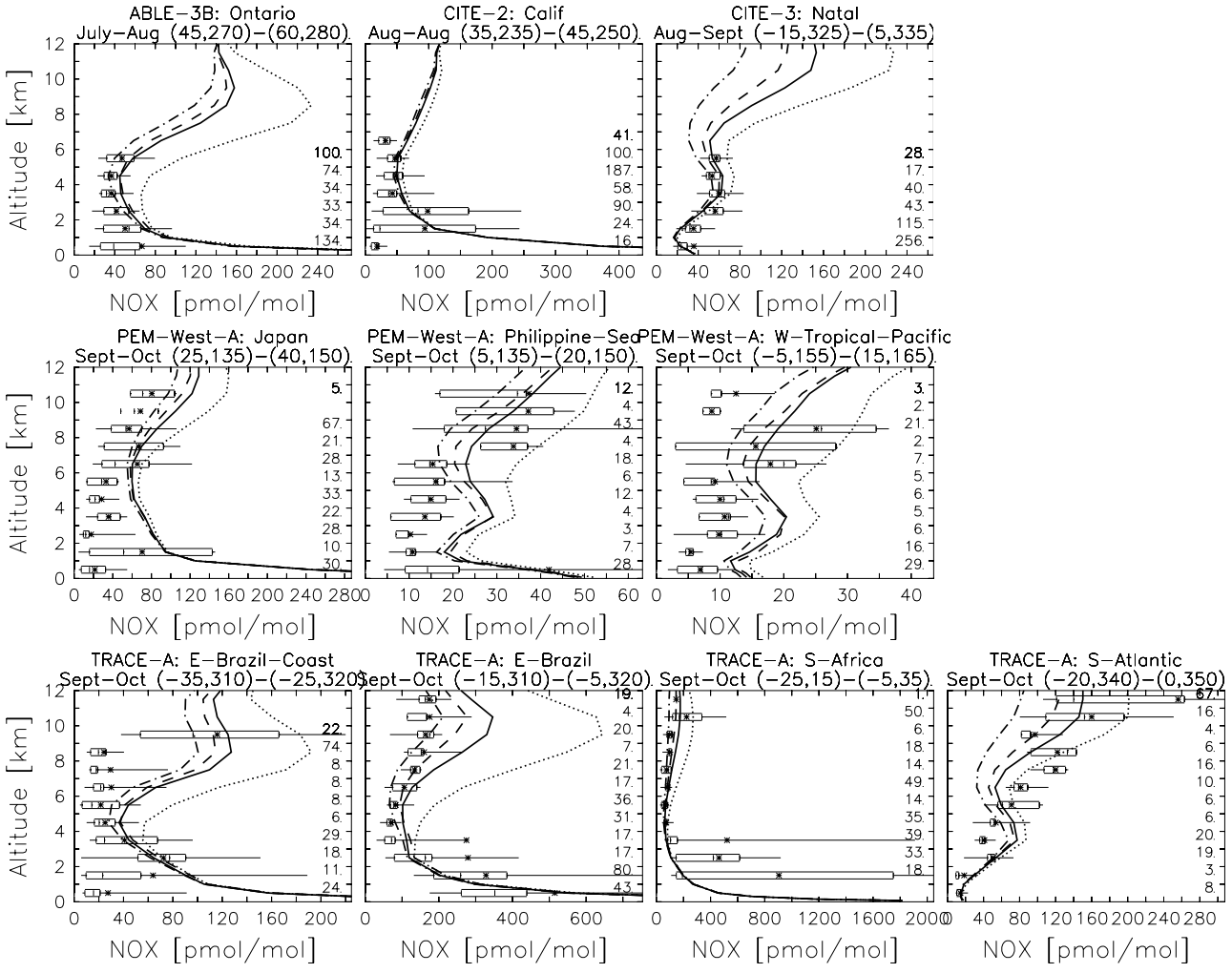

Fig. 12. NO_x profiles for different campaign regions (whisker boxes) and for the NoLtNO_x (dash-dotted line), EVEN5(dashed line), PICK5(solid line) and PICK20 (dotted line) runs. The boxes and whiskers contain the central and side 40% of the observations. On the right-hand side are the number of observations at each altitude. Inside the whisker boxes, the median and mean values are represented by an asterisk and vertical line, respectively.

the 2 and 5 Tg(N)/yr runs in both the PICK and EVEN distributions over the whole globe as well as in the tropics. For higher production rates, the approximately linear response continues without abatement until the top of the production range for both sets of runs, with enhancements of over 100% and 200% over the whole globe and tropics, respectively, in the PICK20 run. This sensitivity increases with the magnitude of the source of NO_x from lightning (Table 4) and is due to the increase in its two main precursors, NO_2 and OH. From Fig. 10d, it is readily apparent that the burdens for the tropical and extratropical regions are very approximately the same; this is in part accounted for by the fact that the OH radical is more abundant in the tropics (see Table 5), while NO_2 is more abundant in the extratropics.

Figure 10e shows that the burden of PAN can be doubled versus the NoLtNO_x run in the tropical UT by assuming the PICK vertical distribution. For every 5 Tg(N)/yr of NO_x from lightning, PAN is enhanced by almost 52% between the NoLtNO_x and PICK5 runs, or about 14% more than NO_x (Table 4). Then, for every additional 5 Tg(N)/yr, PAN is enhanced by 17% between the PICK10 and 20 runs, or about half the increase in NO_x for the same range; thus, the tendency towards saturation is much stronger for PAN than for other trace gases. The strong response at the lower end of the LtNO_x production range in the tropics can be accounted for by the very strong emissions of isoprene in MATCH-MPIC runs in the tropics (von Kuhlmann et al., 2004). The formation of PAN depends, among other factors, on the availability of the peroxyacetyl radical, the dominant producer of which in our runs in the tropical regions is isoprene. As LtNO_x is further increased, however, one moves into a hydrocarbon-limited PAN formation regime. While NO_x is increased

Table 6. Set of campaign regions, campaigns names and coordinates used in this study to compare against model output.

Region	Region name	campaign	Date	Coordinates, deg.
1	Africa-South	TRACE-A	21 Sept.–26 Oct. 1992	25 S–5 S, 15–35
2	Atlantic-S	TRACE-A	21 Sept.–26 Oct. 1992	20 S–0, 340–350
3	Natal	CITE-3	22 Aug.–29 Sept. 1989	15 S–5 N, 325–335
4	E-Brazil	TRACE-A	21 Sept.–26 Oct. 1992	15 S–5 S, 310–320
5	E-Brazil Coast	TRACE-A	21 Sept.–26 Oct. 1992	35 S–25 S, 310–320
6	Ontario	ABLE3-B	6 July–15 Aug. 1990	45 N–60 N, 270–280
7	California	CITE-2	11 Aug.–5 Sept. 1986	35 N–45 N, 235–250
8	Pacific-Tropics-W	PEM-West-A	16 Sept.–21 Oct. 1991	5 S–15 N, 155–165
9	Philippine-sea	PEM-West-A	16 Sept.–21 Oct. 1991	5 N–20 N, 135–150
10	Japan-Coast-E	PEM-West-A	16 Sept.–21 Oct. 1991	15 N–40 N, 135–150

through $LtNO_x$, isoprene emissions, and other PAN precursors are kept constant in our runs, leading to the rapid saturation signal.

6 Comparisons with observations

In this section we compare the model output from the sensitivity runs with a subset of the composites of airborne field campaign observations compiled by Emmons et al. (2000). Table 6 and Fig. 11 show the selected set of observation campaign regions for comparison with our model results. Six regions were selected for their location within the tropics, which are representative of both maritime (Regions 2, 8 and 9 in Fig. 11), continental (Regions 1 and 4) as well as coastal areas (Region 3). Regions 2 and 3 are of particular importance since they are located downwind of NO_x sources such as $LtNO_x$ and biomass burning from the African continent. Four regions were selected in the extratropics, of which two in coastal areas (Regions 5 and 10), and two in continental areas (Region 6 and 7). It bears keeping in mind that the years of the campaigns generally do not coincide with the year of our simulation; this introduces a further element of uncertainty which may need to be assessed in the future in the light of interannual variability of lightning. Figure 12 shows the vertical profiles of NO_x for the measurements of each campaign region plotted (box-whiskers plots) as well as those of the model output for the $NoLtNO_x$, EVEN5, PICK5 and PICK20 runs for the selected regions.

In all but one case, the PICK20 run overestimates the observed NO_x profiles, particularly over the tropical sites. In the case of Regions 3 and 4, the modeled concentrations can be up to a factor of 3 higher than those of the observations at the higher altitudes. While the trend is not as strong over the tropical marine sites (Regions 8 and 9), it is still evident. Over the midlatitudes, where measurements were available (Region 10), the same tendency is again observed, with the PICK20 modeled concentrations about 50% higher than the observed ones. Although more observations are needed, our results give a strong indication that the 20 Tg(N)/yr production of NO_x from lightning is too high a source magnitude.

Other than in the PICK20 run, it is difficult to discern any particular trend of over or underestimation of the model results, even when dividing the comparison between tropics and extratropics. Over the tropical continental landmasses, there is generally good agreement between modeled results and observations in the first 4 km for all 4 areas (Regions 1, 3, 4 and 5) considered. However, there is also little difference between the different model profiles up to that height, which underscores the fact that the largest differences in NO_x mixing ratios are found in the UT (see Fig. 3a). The runs start to exhibit larger differences among themselves above about 4 km. In Region 4, the PICK20 run shows a clear tendency to overestimate above ∼3 km as do, to a much lesser extent, the two runs with 5 Tg(N)/yr production rate. In South Africa (Region 1), the model results tend to underestimate NO_x in the LT, probably as result of underestimated biomass-burning emissions in the model, but there is a slightly better agreement in the free and upper troposphere. The overall low mixing ratios in the UT for both measurements and model results indicate low lightning activity over the campaign region at that time. Even then, the PICK20 run clearly overestimates NO_x in the UT. NO_x measurement above Natal, Brazil (Region 3) were only made for the first 5 km and, up to that height, the PICK5 run shows the best agreement with the observations. Over the two maritime regions in the tropical Pacific Ocean (Regions 8 and 9), all 4 runs plotted tend to clearly overestimate NO_x mixing ratios in the first 4–6 km, probably as a result of excessive downward transport of NO_x-rich air into the lower reaches of the marine troposphere on the part of the model. Above that, there is a better agreement between the runs and the measurements, with the exception of the PICK20 run clearly being on the higher end (when not outside) of the measured values. However, since in the UT the range of measured values is wide and includes the values for most of the model runs, is it not possible to single out any run as having the best agreement. Region 2, in the tropical

south Atlantic, shows a much clearer separation of the profiles for the different runs. Since one would not expect much lightning activity there, this is an indication of transport of NO_x-rich air form the African continent and underscores the importance of long-range transport of trace gases. In the lowermost troposphere and up to 4 km, most runs overestimate measured values, a probable result of excessive PAN in the model as diagnosed before (von Kuhlmann et al., 2003b). The NoLtNO_x run clearly underestimates the measured values in the UT and, while the EVEN5 and PICK20 runs are still within the observed range there, it is the PICK5 run that more closely reproduces observed values. In the middle troposphere, between 4 and 8 km, most runs tend to underestimate measured values.

Over the extratropical continental areas (Regions 6 and 7), measurements were not carried out above 6 km, where the simulated values start to spread. Over Region 6, all runs overestimate NO_x in the first 2 km, as does the PICK20 run for the entire altitude range. The rest of the runs show a better agreement in the free troposphere but, again, no particular run shows better agreement with measured values than the rest. The NO_x profile over Japan (Region 10) shows most runs overestimating NO_x, particularly in the lower and middle troposphere. All 4 runs show very little differences among them at that height, which indicates low flash activity over the region and might point towards other sources than LtNO_x, such as excessive PAN decomposition (von Kuhlmann et al., 2003b), that could be responsible for the disagreement. The coastal area of Brazil (Region 5) shows a clearer separation between all modeled NO_x profiles above 4km, indicating strong lightning activity. Above that height, all 4 runs overestimate NO_x up until 10 km height, when measurements and modeled results (except the PICK20 run) agree again. Pickering et al. (1996) points out that convection was unusually active during the TRACE A campaign in Brazil. The fact that all but the NoLtNO_x run overestimate NO_x in that region suggest that the lightning production in our model may be biased high there. This could be a further indication of PR92's tendency to overestimate lightning over the tropical continents. The vertical profile plots show that, in general, the combination of factors, such as the lack of measurements above 4–5 km, and in key regions such as the tropical continents and the fact that many of the campaigns in the dataset did not specifically target LtNO_x, preclude us from singling out a vertical distribution as "best".

Figure 13 shows the total NO_x scatterplots for 3 runs in this study, namely the NoLtNO_x, PICK5 and PICK20 runs for data above 5 km. The plots are done for the entire set of airborne observation campaigns, comprising 34 regions, in the Emmons et al. (2000) dataset where NO_x measurements are available. The 5 km lower limit was chosen because, as seen from the vertical profile plots, it is where the values for the different runs generally start to separate. The NoLtNO_x run shows a distinct trend to underestimate observed values throughout the entire concentration range, but particularly in

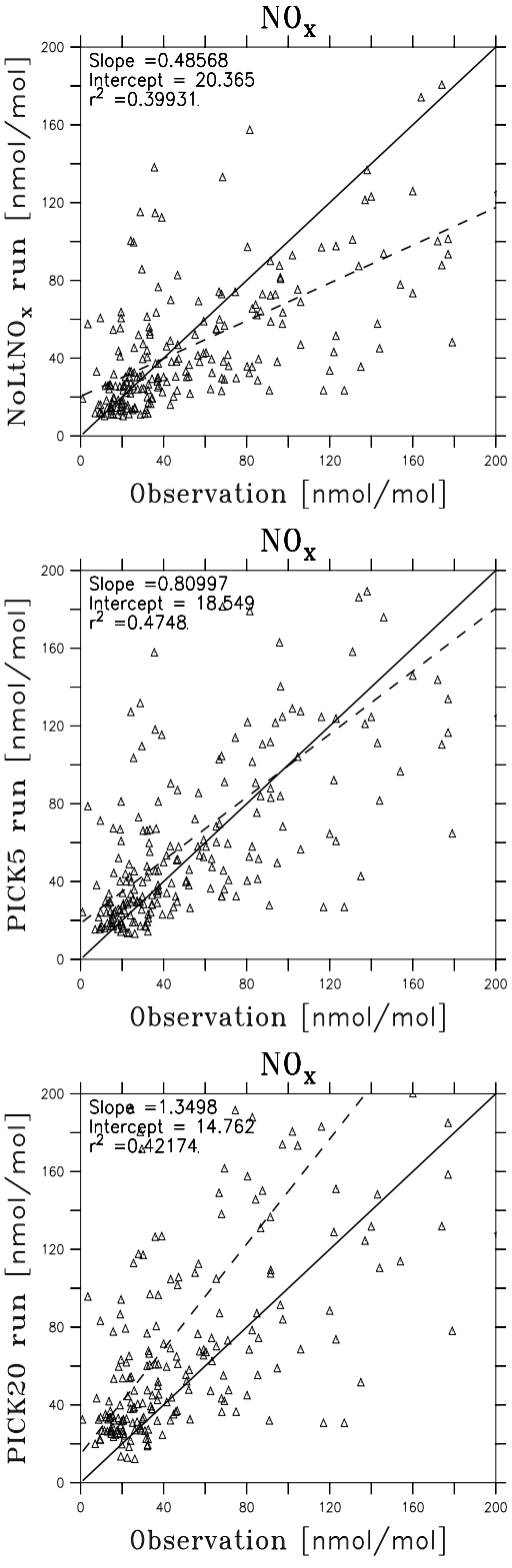

Fig. 13. Scatter plots of the NoLtNO_x, PICK5 and PICK20 runs against airborne observation campaign data above 5km.

the upper range. The PICK5 run shows the best fit of all runs, both burden- and distribution wise, although the EVEN5 run (not pictured) resulted in a very similar correlation coefficient (r^2=0.4655) and a lower slope (0.65866). It is interesting to notice that, in spite of the EVEN5 and PICK5 runs having markedly different NO_x vertical distributions, the difference in the scatter plots is small. We believe this to be due to the lack of observation at key locations where the largest differences could be expected. On the other hand, the PICK20 run shows a clear tendency to overestimate the observations data throughout the entire range, particularly at the upper end, confirming the tendency already seen in the vertical profile plots.

The effects of the vertical distribution and source magnitude of $LtNO_x$ have been addressed before in a number of modeling studies. Tie et al. (2001) and Stockwell et al. (1999) point out that including lightning-NO_x emissions in their models produces better agreement with observations. In another study, Tie et al. (2002) conclude, based on vertical profile plots, that simulations with a production of 7 Tg(N)/yr of NO_x from lightning uniformly distributed in clouds, and 3.5 Tg(N)/yr in the upper regions of clouds produce the best agreement with observations. The differences between our modeled results and the latter study are notable. While there may be many factors to account for this, including the use of different models, we believe that the use of the Hack (1994) convection scheme in Tie et al. (2002) is fundamental in accounting for these differences since it is unable to simulate deep convective mixing well. From our results, it is apparent that it is not possible, based on vertical profiles alone, to arrive at a solid conclusion as to which production rate or vertical distribution yields the best agreement with observations, and while the scatter plots afford an extra measure of objectivity to our analysis, we can only state with a certain degree of confidence that in our simulations the $NoLtNO_x$ and PICK20 runs underestimate and overestimate, respectively, the observations enough not to be considered as realistic assumptions. We believe that the combination of the low availability of observational data, particularly in critical areas, such as the continental tropics, the large scatter in the available observations and the many uncertainties in modeling lightning NO_x and other NO_x sources calls for exercising caution when coming to conclusions about its source magnitude based on simple comparisons with observations. More observations campaigns, such as TROCCINOX (http://www.pa.op.dlr.de/troccinox), specifically aimed at reducing the uncertainties in the source of NO_x from lightning and in key regions, such as the tropical continents, are therefore needed.

7 Conclusions

We have investigated the effects of different assumptions concerning the source magnitude and vertical placement of lightning-produced NO_x on total NO_x as well as on O_3, OH, HNO_3 and PAN using the chemical transport model MATCH-MPIC. Our results show these trace gases to be very sensitive to both parameters. Global increases in NO_x in the tropics compared to a run with no NO_x from lightning are simulated assuming a 5 Tg(N)/yr $LtNO_x$ production rate and a vertical distribution according to Pickering et al. (1998). Since these enhancements occur primarily in the tropical upper troposphere, the produced NO_x, along with all other trace gases resulting from its chemistry, have the potential to be transported over long distances to pristine areas, greatly enhancing concentrations in those places. However, under the present circumstances, we believe that the uncertainties in our knowledge of the production of NO_x from lightning, such as 1) the horizontal distribution of lightning, which we address in a separate study, 2) the energy produced by each type of discharge and number of NO molecules per unit energy, along with 3) the low number of observation campaigns available, make it extremely difficult to determine a "best" vertical distribution and source magnitude. We can say, however, that our results point towards a 0 Tg(N)/yr source of NO_x from lightning as being too low and 20 Tg(N)/yr as being too high. This underscores the need for further measurement campaigns, particularly in the tropical continental regions, where lightning activity is prevalent. On the other hand, there is a definite need for improved lightning parameterizations for use in 3D global chemistry transport models, although substantial improvements in these parameterizations may have to wait until more detailed data are available from next generation convection parameterizations (K. A. Pickering, personal communication, 2004).

Edited by: J. Brandt

References

Allen, D. and Pickering, K.: Evaluation of lightning flash rate parameterizations for use in a global chemical transport model, J. Geophys. Res., 107, 4711, doi:10.1029/2002JD002066, 2002.

Chameides, W., Stedman, D., Dickerson, R., Rusch, D., and Cicerone, R.: NO_x production in lightning, J. Atmos. Sci., 34, 143–149, 1977.

Chameides, W. L.: Production of CO, H_2, and other trace gases by atmospheric lightning, Transactions, Amer. Geophys. Un., 59, 1150–1150, 1979.

Chameides, W. L., Davis, D. D., Bradshaw, J., Rodgers, M., Sandholm, S., and Bai, D. B.: An estimate of the NO_x production-rate in electrified clouds based on NO observation from the GTEs CITE-1 fall 1983 field operation, J. Geophys. Res., 92, 2153–2156, 1987.

Christian, H. J., Blakeslee, R. J., Boccippio, D. J., Boeck, W. L., Buechler, D. E., Driscoll, K. T., Goodman, S. J., Hall, J. M., Koshak, W. J., Mach, D. M., and Stewart, M. F.: Global frequency and distribution of lightning as observed from space

by the optical transient detector, J. Geophys. Res., 108, 4005, doi:10.1029/2002JD002347, 2003.

Cooray, V.: Energy disipation in lightning flashes, J. Geophys. Res., 102, 21 401–21 410, 1997.

Dawson, G. A.: Nitrogen-fixation by lightning, J. Atmos. Sci., 37, 174–178, 1980.

DeCaria, A. J., Pickering, K. E., Stenchikov, G. L., Scala J. R., Stith, J. L., Dye, J. E., and Laroche, B. A. R. P.: A cloud-scale model study of lightning-generated NO_x in an individual thunderstorm during STERAO-A, J. Geophys. Res., 105, 11 601–11 616, 2000.

Drapcho, D. L., Sisterson, D., and Kumar, R.: Nitrogen fixation by lightning activity in a thunderstorm, J. Geophys. Res., 19, 729–734, 1983.

Emmons, L. K., Hauglustaine, D. A., Müller, J.-F., Carroll, M. A., Brasseur, G. P., Brunner, D., Staehelin, J., Thouret, V., and Marenco, A.: Data composites of airborne observations of tropospheric ozone and its precursors, J. Geophys. Res., 105, 20 497–20 538, 2000.

Fehr, T., Höller, H., and Huntrieser, H.: Model study on production and transport of lightning-produced NO_x in a EULINOX supercell storm, J. Geophys. Res., 109, D09 102, doi:10.1029/2003JD003935, 2004.

Franzblau, E. and Popp, C. J.: Nitrogen oxides produced from lightning, J. Geophys. Res., 94, 11 089–11 104, 1989.

Gallardo, L. and Cooray, V.: Could cloud-to-cloud discharges be as effective as cloud-to-ground discharges in producing NO_x?, Tellus, 48B, 641–651, 1996.

Goldenbaum, G. C. and Dickerson, R. R.: Nitric-oxide production by lightning discharges, J. Geophys. Res., 98, 18 333–18 338, 1993.

Hack, J. J.: Parameterization of moist convection in the National Center for Atmospheric Research community climate model (CCM2), J. Geophys. Res., 99, 5551–5568, 1994.

Hill, R. D., Rinker, R. G., and Wilson, H. D.: Atmospheric nitrogen-fixation by lightning, J. Atmos. Sci., 37, 179–192, 1980.

Huntrieser, H., Feigl, C., Schlager, H., Schröder, F., Gerbig, C., van Velthoven, P., Flatøy, F., Thery, C., Petzold, A., Höller, H., and Schumann, U.: Airborne measurements of NO_x, tracer species, and small particles during the European Lightning Nitrogen Oxides Experiment, J. Geophys. Res., 107, 4113, doi:10.1029/2000JD000209, 2002.

Kowalczyk, M. and Bauer, E.: Lightning as a source of NO_x in the troposphere, Technical Memorandum ORNL/TM-2001/268, Federal Aviation Administration, Oak Ridge, Tenn., 1982.

Kumar, P. P., Manohar, G. K., and Kandalgaonkar, S. S.: Global distribution of nitric-oxide produced by lightning and its seasonal variation, J. Geophys. Res., 100, 11 203–11 208, 1995.

Labrador, L., von Kuhlmann, R., and Lawrence, M. G.: Strong sensitivity of the global mean OH concentration and the tropospheric oxidizing efficiency to the source of NO_x from lightning, Geophys. Res. Lett., 31, L06 102, doi:10.1029/20 003GL019 229, 2004.

Lawrence, M. G., Chameides, W. L., Kasibhatla, P. S., Levy II, H., and Moxim, W.: Lightning and atmospheric chemistry: The rate of atmospheric NO production, Vol. I, pp. 189–202, CRC Press, Inc., 1995.

Lawrence, M. G., Crutzen, P. J., Rasch, P. J., Eaton, B. E., and Mahowald, N. M.: A model for studies of tropospheric photochemistry: Description, global distributions, and evaluation, J. Geophys. Res., 104, 26 245–26 277, 1999.

Lawrence, M. G., Jöckel, P., and von Kuhlmann, R.: What does the global mean OH concentration tell us?, Atmos. Chem. Phys., 1, 37–49, 2001,
SRef-ID: 1680-7324/acp/2001-1-37.

Lawrence, M. G., Rasch, P. J., von Kuhlmann, R., Williams, J., Fischer, H., de Reus, M., Lelieveld, J., Crutzen, P. J., Schultz, M., Stier, P., Huntrieser, H., Heland, J., Stohl, A., Forster, C., Elbern, H., Jakobs, H., and Dickerson, R. R.: Global chemical weather forecasts for field campaign planning: predictions and observations of large-scale features during MINOS, CONTRACE, and INDOEX, Atmos. Chem. Phys., 3, 267–289, 2003a,
SRef-ID: 1680-7324/acp/2003-3-267.

Lawrence, M. G., von Kuhlmann, R., and Salzmann, M.: The balance of effects of deep convective mixing on tropospheric ozone, Geophys. Res. Lett., 30, 1940, doi:10.1029/2003GL017644, 2003b.

Levine, J. S., Rogowski, R. S., Gregory, G. L., Howell, W. E., and Fishman, J.: Simultaneous measurements of NO_x, NO and O_3 production in a laboratory discharge: Atmospheric implications, Geophys. Res. Lett., 8, 357–360, 1981.

Levy, H., Moxim, W. J., and Kasibhatla, P. S.: A global three-dimensional time-dependent lightning source of tropospheric NO_x, J. Geophys. Res., 101, 22 911–22 922, 1996.

Liaw, Y. P., Sisterson, D. L., and Miller, N. L.: Comparison of field, laboratory, and theoretical estimates of global nitrogen-fixation by lightning, J. Geophys. Res., 22, 22 489–22 494, 1990.

Navarro-Gonzales, R., Villagran-Muniz, M., Molina, L., and Molina, M.: The physical mechanism of nitric oxide formation in simulated lightning, Geophys. Res. Lett., 28, 3867–3870, 2001.

Nesbitt, S. W., Zhang, R., and Orville, R. E.: Seasonal and global NO_x production by lightning estimated from the Optical Transient Detector (OTD), Tellus, 52B, 1206–1215, 2000.

Noxon, J. F.: Atmospheric nitrogen-fixation by lightning, Geophys. Res. Lett., 3, 463–465, 1976.

Peyrous, R. and Lapyere, R. M.: Gaseous products created by electrical discharges in the atmosphere and condensation nuclei resulting from gaseous-phase reactions, Atmos. Environ., 6, 959–968, 1982.

Pickering, K. E., Thompson, A. M., Wang, Y., Tao, W.-K., McNamara, E. P., Kichhoff, V. W. J. J., Heikes, B. G., SAchse, G. W., Bradshaw, J. D., Gregory, G. L., and Blake, D. R.: Convective transport of biomass burning emissions over Brazil during TRACE A, J. Geophys. Res., 101, 23 993–24 012, 1996.

Pickering, K. E., Wang, Y., Tao, W. K., Price, C., and Müller, J.-F.: Vertical distributions of lightning NO_x for use in regional and global chemical transport models, J. Geophys. Res., 103, 31 203–31 216, 1998.

Price, C. and Rind, D.: A simple lightning parameterization for calculating global lightning distributions, J. Geophys. Res., 97, 9919–9933, 1992.

Price, C. and Rind, D.: Modeling global lightning distributions in a general circulation model, Mon. Weather Rev., 122, 1930–1939, 1994.

Price, C., Penner, J., and Prather, M.: NO_x from lightning: 1. Global distribution based on lightning physics, J. Geophys. Res., 102, 5929–5941, 1997a.

Price, C., Penner, J., and Prather, M.: NO_x from lightning: 2. Constraints from the global atmospheric electric circuit, J. Geophys.

Res., 102, 5942–5951, 1997b.

Rasch, P. J., Mahowald, N. M., and Eaton, B. E.: Representations of transport, convection and the hydrologic cycle in chemical transport models: Implications for the modeling of short lived and soluble species, J. Geophys. Res., 102, 28 127–28 138, 1997.

Ridley, B., Ott, L., Pickering, K., Emmons, L., Montzka, D., Weinheimer, A., Knapp, D., Grahek, F., Li, L., Heymsfeld, G., McGill, M., Kucera, P., Mahoney, M. J., Baumgardner, D., Schultz, M., and Brasseur, G.: Florida thunderstorms: A faucet of reactive nitrogen to the upper troposphere, J. Geophys. Res., 109, doi:10.1029/2004JD004769, 2004.

Ridley, B. A., Dye, J. E., Walega, J. G., Zheng, J., Grahek, F. E., and Rison, W.: On the production of active nitrogen by thunderstorms over New Mexico, J. Geophys. Res., 101, 20 985–21 005, 1996.

Sisterson, D. L. and Liaw, Y. P.: An evaluation of lightning and corona discharge on thuderstorm air and precipitation chemistry, J. Atmos. Chem., 10, 83–96, 1990.

Stockwell, D. Z., Giannakopoulos, C., Plantevin, P. H., Carver, G. D., Chipperfield, M. P., Law, K. S., Pyle, J. A., Shallcross, D. E., and Wang, K.-Y.: Modelling NO_X from lightning and its impact on global chemical fields, Atmos. Environ., 33, 4477–4493, 1999.

Tie, X., Brasseur, G., Emmons, L., Horowitz, L., and Kinnison, D.: Effects of aerosols on tropospheric oxidants: A global model study, J. Geophys. Res., 106, 22 931–22 964, 2001.

Tie, X., Zhang, R., Brasseur, G., and Lei, W.: Global NO_X production by lightning, J. Atmos. Chem., 43, 61–74, 2002.

Tuck, A. F.: Production of nitrogen-oxides by lightning discharges, Q. J. R. Meteorol. Soc., 102, 749–755, 1976.

Turman, B. N.: Analysis of lightning data from DMSP satellite, J. Geophys. Res., 83, 5019–5024, 1978.

von Kuhlmann, R., Lawrence, M. G., Crutzen, P. J., and Rasch, P. J.: A model for studies of tropospheric ozone and nonmethane hydrocarbons: Model description and ozone results, J. Geophys. Res., 108, 4294, doi:10.1029/2002JD002893, 2003a.

von Kuhlmann, R., Lawrence, M. G., Crutzen, P. J., and Rasch, P. J.: A model for studies of tropospheric ozone and non-methane hydrocarbons: Model evaluation of ozone related species, J. Geophys. Res., 108, 4729, doi:10.1019/2002JD003348, 2003b.

von Kuhlmann, R., Lawrence, M. G., Pöschl, U., and Crutzen, P. J.: Sensitivities in global scale modeling of isoprene, Atmos. Chem. Phys., 4, 1–17, 2004,
SRef-ID: 1680-7324/acp/2004-4-1.

von Liebig, J.: Extrait d'une note sur la nitrification, Ann. Chem. Phys., 35, 329–333, 1827.

Wang, Y., DeSilva, A. W., Goldenbaum, G. C., and Dickerson, R. R.: Nitric oxide production by simulated lightning: Dependence on current, energy, and pressure, J. Geophys. Res., 103, 19 149–19 159, 1998.

Zhang, G. J. and McFarlane, N. A.: Sensitivity of climate simulations to the parameterization of cumulus convection in the canadian climate centre general circulation model, Atmos. Ocean, 33, 407–446, 1995.

Zhang, R., Tie, X., and Bond, D. W.: Impacts of anthropogenic and natural NO_X sources over the U.S. on tropospheric chemistry, Proc. Nat. Acad. of Sci., 100, 1505–1509, 2003a.

Zhang, X. J., Helsdon Jr., J. H., and Farley, R. D.: Numerical modeling of lightning-produced NO_X using and explicit lightning scheme: 1. Three-dimensional simulation and expanded chemistry, J. Geophys. Res., 108, 4580, doi:10.10.1029/2002JD003225, 2003b.